FBXO45-MYCBP2 regulates mitotic cell fate by targeting FBXW7 for degradation

Kai T. Richter, Yvonne T. Kschonsak[#], Barbara Vodicska[#] and Ingrid Hoffmann*

Cell Cycle Control and Carcinogenesis, F045, German Cancer Research Center, DKFZ, Im Neuenheimer Feld 242, 69120 Heidelberg, Germany

[#]These authors contributed equally

*Correspondence: Ingrid.Hoffmann@dkfz.de

SUMMARY

Cell fate decision upon prolonged mitotic arrest induced by microtubule targeting agents depends on the activity of the tumor suppressor and F-box protein FBXW7. FBXW7 promotes mitotic cell death and prevents premature escape from mitosis through mitotic slippage. Mitotic slippage is a process that can cause chemoresistance and tumor relapse. Therefore, understanding the mechanisms that regulate the balance between mitotic cell death and mitotic slippage is an important task. Here we report that FBXW7 protein levels markedly decline during extended mitotic arrest. FBXO45 binds to a conserved acidic N-terminal motif of FBXW7 specifically under a prolonged delay in mitosis, leading to ubiquitylation and subsequent proteasomal degradation of FBXW7 by the FBXO45-MYCBP2 E3 ubiquitin ligase. Moreover, we find that FBXO45-MYCBP2 counteracts FBXW7 in that it promotes mitotic slippage and prevents cell death in mitosis. Targeting this interaction represents a promising strategy to prevent chemotherapy resistance.

Key words: FBXW7, ubiquitylation, proteasome, FBXO45, MYCBP2, mitotic slippage, cell fate decision, SCF, mitotic cell death

INTRODUCTION

The attachment of a single ubiquitin molecule or a polyubiquitin chain to a eukaryotic protein is an essential signaling event that can profoundly affect the fate of the target protein. For example, the ubiquitin-proteasome system controls protein degradation in a broad array of cellular processes (Hershko and Ciechanover, 1998). Cancer cells often contain mutations targeting ubiquitin-mediated proteolysis that lead to tumorigenesis. FBXW7, an F-box protein and substrate receptor for the SCF (SKP1-CUL1-F-box protein) E3 ubiquitin ligase complex, acts as a tumor suppressor and is mutated or deleted in a variety of human cancers (Davis et al., 2014). FBXW7 exerts its anti-tumor activity through destruction of key oncoproteins, including JUN (Nateri et al., 2004) (Wei et al., 2005), MYC (Welcker et al., 2004) (Yada et al., 2004), Cyclin E (Koepp et al., 2001) (Moberg et al., 2001) (Strohmaier et al., 2001) and Notch1 (Hubbard et al., 1997) (Gupta-Rossi et al., 2001).

The abundance of F-box proteins including FBXW7 is controlled by ubiquitylation and degradation in an autocatalytic reaction within the SCF complex (Galan and Peter, 1999). FBXW7 autoubiquitylation can be regulated by Glomulin (GLMN), a protein that binds to RBX1 leading to inhibition of SCF activity, thereby increasing FBXW7 protein levels (Duda et al., 2012) (Tron et al., 2012). The only ubiquitin ligase known to date involved in regulating FBXW7 levels in neurons is Parkin. However, this regulation has only been observed for the FBXW7β isoform (Ekholm-Reed et al., 2013). It has also been shown that PLK2-kinase dependent phosphorylation of FBXW7 at S176 leads to its ubiquitin-mediated degradation and stabilization of Cyclin E (Cizmecioglu et al., 2012).

Accurate spindle function is crucial for a successful mitosis. Perturbation of microtubule dynamics leads to sustained activation of the spindle assembly checkpoint (SAC) (Rieder and Maiato, 2004). The SAC delays exit from mitosis by preventing the anaphase-promoting complex/cyclosome (APC/C) mediated proteolysis of Cyclin B1. Anti-cancer chemotherapeutics including vinca alkaloids or taxanes target microtubules and are successfully used in the clinics to treat multiple types of cancer. Anti-microtubule drugs cause an arrest or prolonged delay in mitosis followed by mitotic cell death. On the

other hand, slow degradation of Cyclin B1 during a prolonged mitotic arrest can cause cells to prematurely exit from mitosis, a process called mitotic slippage (Brito and Rieder, 2006). During mitotic slippage, cells do not undergo proper chromosome segregation and cytokinesis. Most of the resulting tetraploid cells either undergo cell death after mitosis or arrest in interphase. However, depending on the p53 status of these cells, they may continue to proliferate as genomically unstable cells. This can lead to chemoresistance, thereby limiting the therapeutic use of anti-microtubule drugs (Frederiks et al., 2015) (Haschka et al., 2018). FBXW7 is a known regulator of mitotic cell fate. Upon mitotic arrest, FBXW7 promotes mitotic cell death and prevents mitotic slippage (Finkin et al., 2008) (Wertz et al., 2011).

FBXO45 (FSN-1 in *C. elegans*; DFsn in *Drosophila melanogaster*) is an evolutionary conserved F-box protein. FBXO45 is atypical in that it binds to SKP1 via its F-box motif, but recruits an alternate RING-finger protein known as MYCBP2, a member of the PHR (PAM/Highwire/RPM-1) protein family and E3 ubiquitin ligase. MYCBP2 was shown to have important functions in developmental processes, such as axon termination and synapse formation, as well as axon degeneration (reviewed by (Grill et al., 2016) (Po et al., 2010)). FBXO45 contains a conserved F-box domain and a SPRY domain, which recruits substrates to the ubiquitin ligase complex (Chen et al., 2014) (Kugler et al., 2010). FBXO45-MYCBP2 has been linked to the proteasomal degradation of a few targets including the DLK-1 and p38 MAP kinase pathway (Nakata et al., 2005) and the nicotinamide-nucleotide adenylyltransferase family member NMNAT (Xiong et al., 2012).

Here we report the identification of the E3 ligase FBXO45-MYCBP2 as a regulator of FBXW7 abundance during prolonged mitotic arrest induced by spindle poisons. FBXO45 binds to a conserved acidic N-terminal region of FBXW7. Depletion of FBXO45 leads to stabilization of FBXW7 protein upon mitotic arrest. Ubiquitylation of FBXW7 by FBXO45-MYCBP2 induces its proteasomal degradation inducing an increase in mitotic slippage and prevention of mitotic cell death.

RESULTS

The FBXO45-MYCBP2 complex binds to a conserved N-terminal motif in FBXW7α

The SCF-FBXW7 complex acts as a key factor determining sensitivity to anti-mitotic drugs in cancer by inducing mitotic cell death and preventing mitotic slippage (Allan et al., 2018) (Wertz et al., 2011) (Finkin et al., 2008). As mitotic slippage frequently occurs under prolonged mitotic arrest, it is conceivable that this could be induced by a decrease in FBXW7 protein levels. To address this, we analyzed protein levels of the ubiquitously expressed α-isoform of FBXW7 in mitotic HeLa cells at different time points after induction of mitotic arrest. We observed a slow but gradual decrease in the amount of FBXW7 protein during prolonged mitotic arrest (Figure 1A) similar to the decay of Cyclin B1 and MCL-1 under mitotic arrest (Brito and Rieder, 2006) (Harley et al., 2010), which was prevented by the addition of the proteasomal inhibitor MG132 (Figure S1A). We therefore anticipated that FBXW7 protein levels could be decreased in response to proteasomal protein degradation. To identify proteins that regulate SCF-FBXW7 protein levels we made use of an unbiased screen where we aimed at identifying FBXW7 binding proteins. We expressed Flag-FBXW7α in HEK-293T cells, FBXW7α complexes were immunoprecipitated and subsequent mass spectrometrical analysis was performed. Among the identified peptides were sequences corresponding to FBXO45 and MYCBP2, along with SCF components and known substrates of FBXW7 including MYC, Notch1/2 and members of the mediator complex (Table S1). Interestingly, FBXO45 and MYCBP2 have previously been identified in other screens for FBXW7 interacting proteins (Kourtis et al., 2015) (Huttlin et al., 2017). They have also been described to form an SCF-like E3 ubiquitin ligase complex (Liao et al., 2004).

We then analyzed whether FBXO45-MYCBP2 is the ubiquitin ligase that regulates FBXW7 protein levels under prolonged mitotic arrest. First, we aimed to confirm the binding between FBXW7 and FBXO45. We therefore expressed Flag-FBXO45 in HEK-293T cells and immunoprecipitated the protein with α-Flag-resin. We found that Flag-FBXO45 was able to co-immunoprecipitate endogenous FBXW7α (Figure 1B). FBXW7 occurs in three

isoforms, FBXW7α, FBXW7β and FBXW7γ, that differ in subcellular localization and their N-terminal domain. FBXW7α is thought to perform most FBXW7 functions (Davis et al., 2014). To identify the binding site of FBXO45 within FBXW7 we generated different FBXW7α truncated versions and found that aa106-126 in the N-terminal domain of FBXW7α were required for FBXO45 binding (Figure S1B-D). Co-immunoprecipitation experiments using full-length Flag-FBXW7α or a Flag-FBXW7αΔ106-126 mutant showed that FBXW7αΔ106-126 failed to bind FBXO45 and MYCBP2 (Figure 1C). This could be confirmed by the fact that FBXO45 only interacted with FBXW7α but not with the other two isoforms, FBXW7β or FBXW7γ (Figure S1E), that lack the FBXW7α-specific N-terminal domain (Welcker and Clurman, 2008). Interestingly, the N-terminal stretch within the FBXW7α isoform (aa106-126) harbors conserved acidic amino acid residues as a potential FBXO45 interaction domain (Figure 1D). On other the hand, we identified the central domain of MYCBP2 (aa1951-2950) to be responsible for FBXW7α binding (Figure S1F-G). As this domain also contains the FBXO45 interaction site of MYCBP2, we hypothesized that FBXO45 could be the direct interaction partner of FBXW7α within the FBXO45-MYCBP2 complex. Analysis of binding between purified MBP-tagged N-terminal domain of FBXW7α (MBP-FBXW7α-N167) and *in vitro* translated [^{35}S]-FBXO45 or [^{35}S]-MYCBP2(1951-2950) showed that FBXW7α directly binds to FBXO45 but not to MYCBP2 (Figure 1E). Furthermore, using sequential co-immunoprecipitation experiments we showed that FBXW7α exists in a complex with FBXO45 and MYCBP2 (Figure 1F). Together, these results show that the FBXO45-MYCBP2 complex interacts with a conserved acidic stretch within the N-terminal domain of FBXW7α.

FBXO45-MYCBP2 targets FBXW7α for degradation specifically during mitotic arrest

As FBXW7α is predominantly found in the nucleus (Kimura et al., 2003) whereas FBXO45 and MYCBP2 are cytosolic proteins (Chen et al., 2014) (Pierre et al., 2004) (Figure 2A), a possible interaction between these proteins may occur in mitosis upon nuclear envelope breakdown, when the contents of the cell nucleus are released into the cytoplasm. As FBXO45 is likely to be the

substrate binding factor we analyzed the interaction between Flag-FBXO45 and endogenous FBXW7α in asynchronous and mitotic HeLa cells. The cell extracts for this experiment were generated under conditions where the nucleus remains intact. Interestingly, FBXW7α was specifically found in co-immunoprecipitation with Flag-FBXO45 in mitotic cells (Figure 2B). Furthermore, we noticed an increase in FBXW7α protein levels upon siRNA-mediated downregulation of FBXO45. This effect could only be observed in cells under a prolonged mitotic arrest but not in cells passing through an unperturbed mitosis. In addition, the effect was not observed in asynchronous cells (Figure 2C, Figure S2A-B). On the other hand, FBXW7 downregulation had no effect on FBXO45 protein levels (Figure 2C). To exclude off-target effects we used different FBXO45 and MYCBP2 siRNAs to reduce their expression in HeLa cells and confirmed that FBXW7α protein levels were upregulated in cells that were FBXO45 or MYCBP2-depleted under prolonged mitotic arrest (Figure S2C). The effect could be confirmed in U2OS cells using nocodazole and in HeLa cells using different inhibitors that cause a mitotic arrest (Figure S2D-I). We also aimed to confirm the observed regulation of FBXW7α protein levels by expression of a dominant-negative MYCBP2(1951-2950) fragment that binds FBXO45 and FBXW7α but lacks the RING domain (Figure S1F-G). Upon ectopical expression of Flag-MYCBP2(1951-2950) we found that FBXW7α protein levels were specifically upregulated in mitotic cells after treatment with nocodazole (Figure 2D). Taken together, FBXO45 binds FBXW7α in mitotic cells and the FBXO45-MYCBP2 complex regulates FBXW7α protein levels specifically during mitotic arrest.

FBXO45-MYCBP2 targets FBXW7α for ubiquitylation and degradation

To find out whether the regulation of FBXW7α by FBXO45-MYCBP2 is mediated by ubiquitylation we carried out *in vivo* ubiquitylation assays. We found that both overexpression of FBXO45 and MYCBP2 promote ubiquitylation of FBXW7α (Figure 3A). Deletion of the FBXO45 binding site in FBXW7α reduced the ubiquitylation of FBXW7α markedly in *in vivo* ubiquitylation assays using FBXW7αΔ106-126 expression (Figure 3B). To study the effect of FBXO45 on FBXW7α protein stability, we depleted FBXO45 in nocodazole-treated cells and added cycloheximide to block

translation. Cells were then harvested at different time points after cycloheximide addition. In FBXO45-depleted cells FBXW7α was markedly stabilized (Figure 3C) suggesting that FBXO45 promotes degradation of FBXW7α upon mitotic arrest. In addition, Flag-FBXW7αΔ106-126 was stabilized in comparison to full-length Flag-FBXW7α. The stability of Flag-FBXW7α was increased by MG132 treatment (Figure 3D). From these experiments, we conclude that FBXO45-MYCBP2 mediated degradation of FBXW7α during prolonged mitosis depends on the proteasome.

FBXO45-MYCBP2 reduces the sensitivity of cells to spindle poisons

Previous studies have shown that FBXW7 regulates mitotic cell fate. In fact, FBXW7 promotes mitotic cell death and prevents mitotic slippage in cells that have been treated with anti-microtubule drugs to arrest them in mitosis (Finkin et al., 2008) (Wertz et al., 2011), which is in line with its function as a tumor suppressor. As we had found that FBXO45-MYCBP2 regulates FBXW7α protein levels during mitotic arrest (Figure 2), we asked whether the FBXO45-MYCBP2 complex as a regulator of FBXW7 would also affect mitotic cell fate. To test this, we analyzed mitotic cell fate by live-cell imaging (Figure S3A, Video S1-2). For our live-cell imaging analysis, we treated the cells with spindle poisons at concentrations that completely prevented cell division and caused either mitotic cell death or mitotic slippage (Brito et al., 2008). As shown in Figure 4A, reduction of FBXO45 led to an increase in mitotic cell death in cells that were arrested in mitosis with nocodazole. Similar effects were observed in cells arrested in mitosis by Taxol or vincristine treatment (Figure S3B-C). To exclude off-target effects we used siRNAs targeting different regions of FBXO45 mRNA (Figure 4A). In addition, expression of an siRNA-resistant version of Flag-FBXO45 was able to rescue the effect on mitotic cell fate (Figure 4B). Moreover, siRNA-mediated downregulation of MYCBP2 also caused an increase in mitotic cell death (Figure S3D). In contrast, FBXO45 and MYCBP2 depletion did not have an effect on progression of cells through an unperturbed mitosis (Figure S3E). To verify the results in an siRNA independent approach, we analyzed the effect of the dominant-negative MYCBP2(1951-2950) fragment on mitotic cell fate. As expected, overexpression of Flag-MYCBP2(1951-2950) increased mitotic cell

death (Figure 4C). In addition, we performed a FACS analysis of the DNA content in cells arrested in mitosis. Mitotic slippage leads to the formation of tetraploid cells, which is reflected by an increase in the DNA content. FBXO45 depletion reduced the increase in DNA content, which confirms the negative effect of FBXO45 downregulation on mitotic slippage (Figure 4D, Figure S3F). Taken together, these results showed that the FBXO45-MYCBP2 complex negatively regulates mitotic cell death and increases mitotic slippage, suggesting that it has an opposing function during mitotic arrest compared to FBXW7. This is in line with the FBXO45-MYCBP2 complex being a negative regulator of FBXW7α during mitotic arrest. We therefore asked whether the observed effect of FBXO45-MYCBP2 on mitotic cell fate depends on FBXW7. In fact, FBXW7 depletion was able to rescue the effect of FBXO45, suggesting that FBXW7α is the downstream target of the FBXO45-MYCBP2 complex that mediates mitotic cell fate regulation (Figure 4E). Together, our data strongly suggest that FBXO45-MYCBP2-mediated degradation of FBXW7 under prolonged mitotic arrest induces mitotic slippage and prevents mitotic cell death.

DISCUSSION

The results presented here demonstrate that the FBXO45-MYCBP2 complex is a novel E3 ubiquitin ligase regulating the protein levels of FBXW7α during prolonged mitotic arrest induced by anti-microtubule drugs through ubiquitin mediated degradation. This degradation leads to a reduction of the sensitivity to microtubule-targeting drugs by causing a decrease in mitotic cell death and promoting mitotic slippage.

Prolonged mitotic arrest is caused by a sustained activation of the spindle assembly checkpoint (SAC). If the SAC cannot be satisfied and mitosis cannot be completed, there are two alternative cell fates. Cells either undergo mitotic cell death or perform mitotic slippage. Cell fate following mitotic arrest is regulated by two competing networks, namely Cyclin B1 degradation and pro-apoptotic caspase activation (Gascoigne and Taylor, 2008). Mitotic slippage is promoted by a slow degradation of Cyclin B1 in the presence of an

active SAC during a protracted arrest in metaphase (Brito and Rieder, 2006). Cells undergo mitotic slippage and enter interphase without performing proper chromosome segregation or cytokinesis. The anaphase-promoting complex (APC/C) ubiquitin ligase is known to mediate the degradation of Cyclin B1, but recent data show that an additional E3 ubiquitin ligase, $CRL2^{ZYG11}$, targets Cyclin B1 for degradation in a pathway that facilitates mitotic slippage (Balachandran et al., 2016). Besides cell fate regulation through Cyclin B1, MCL-1, a pro-survival member of the BCL-2 family, was shown to be involved in cell fate decision. MCL-1 is degraded by a ubiquitin-proteasome-dependent mechanism in response to the disruption of mitosis, resulting in cell death (Gascoigne and Taylor, 2008) (Harley et al., 2010) (Wertz et al., 2011).

The tumor suppressor FBXW7 also plays important roles in mitotic cell fate decision (Wertz et al., 2011) (Allan et al., 2018) (Finkin et al., 2008). However, whether or not FBXW7 has a direct role in regulating MCL-1 levels is a matter of debate (Wertz et al., 2011) (Sloss et al., 2016) (Allan et al., 2018) and therefore the identification of the substrate(s) of FBXW7 involved in regulating mitotic cell fate is an important task for future studies.

Our work identifies FBXO45 as a protein binding to a conserved acidic amino acid motif (aa106-126) of FBXW7α (Figure 1) to form a ternary complex with MYCBP2. Interestingly, MYCBP2 has been recently uncovered as a novel type of E3 ligase with esterification activity leading to ubiquitylation of serine and threonine residues in substrates (Pao et al., 2018), which is intrinsic to higher eukaryotes. In the future, it would therefore be interesting to see whether FBXW7 could be ubiquitylated on hydroxyl groups by MYCBP2.

An interesting question that arises is why the regulation of FBXW7α by FBXO45-MYCBP2 can only be observed under a prolonged mitotic arrest but not in cells undergoing a normal mitosis (Figure 2C, Figure S2A-B, Figure S3E). As FBXW7α is a nuclear protein but FBXO45 is found in the cytoplasm (Figure 2A), the two proteins can only interact upon nuclear envelope breakdown (Figure 2B). However, since mitosis is a relatively short process in the eukaryotic cell cycle, the successful formation of a sustained interaction between FBXO45 and FBXW7α may require a longer arrest in mitosis.

In the future, the development of a specific inhibitor to block the FBXO45-MYCBP2-FBXW7α axis might actively promote mitotic cell death and prevent

mitotic slippage. Therefore, treatment of cancer patients with this inhibitor after or in combination with anti-microtubule drugs could be a promising approach in order to increase the efficiency of chemotherapeutic treatment.

MATERIALS AND METHODS

Cell culture and transfection

Human cell lines were grown in a humidified atmosphere with 5% CO_2 at 37°C. HeLa, U2OS and U2OS Flp-In-T-Rex cells were cultured in Dulbecco's Modified Eagle's Medium (DMEM, Sigma-Aldrich) with 1 g/l glucose. HEK-293T cells were grown in DMEM with 4.5 g/l glucose. The media were supplemented with 10% fetal bovine serum (FBS, Sigma-Aldrich or Thermo Scientific). HeLa GFP-α-tubulin/RFP-H2B cells (D. Gerlich, ETH Zürich) were cultured in DMEM containing 1 g/l glucose, 10% FBS, 500 µg/ml G418 and 0.5 µg/ml puromycin. The T-Rex system was used to generate U2OS Flp-In-T-Rex Flag-FBXW7α, U2OS Flp-In-T-Rex Flag-FBXW7αΔ106-126 and U2OS Flp-In-T-Rex Flag-MYCBP2(1951-2950) stable cell lines according to the manufacturer's instructions (Life Technologies).

Cell culture work was performed under sterile conditions. Cell line authentication was regularly performed by Multiplexion in Heidelberg.

HEK-293T and HeLa cells were transiently transfected with plasmid DNA using polyethylenimine (PEI, Polysciences) at a final concentration of 5 µg/ml. The cells were incubated at 37°C and harvested 24-48 h after transfection. If the cells were harvested 48 h after transfection, the transfection mixture was removed 6-24 h after transfection and replaced by fresh growth medium.

For the transfection of HeLa or U2OS cells with siRNA, the transfection reagent Lipofectamine 2000 (Invitrogen) was used according to the manufacturer's instructions. Cells were transfected with 30 nM of siRNA for 72 h. For rescue experiments, 50 ng of plasmid were co-transfected with 40 nM of siRNA for 72 h.

The following siRNA sequences were used:

GL2 (firefly luciferase, control), 5'-CGUACGCGGAAUACUUCGAtt-3';

FBXO45 #1, 5'-GGAGAAAGAAUUCGAGUCAtt-3';

FBXO45 #2, 5'-ACACAUGGUUAUUGCGUAUtt-3';

FBXW7, 5'-ACAGGACAGUGUUUACAAAtt-3';
MYCBP2 #1, 5'-CCCGAGAUCUUGGGAAUAAtt-3'.
FBXO45 #3 (200933, L-023542-01-0005) and MYCBP2 #2 (23077, L-006951-00-0005) were purchased as SMARTpools from Dharmacon. If not stated otherwise, FBXO45 siRNA #2 was used for FBXO45 depletion and MYCBP2 siRNA #2 was transfected in order to downregulate MYCBP2.

Cell cycle synchronization

In order to arrest HeLa or U2OS cells in G1/S phase, the cells were treated with 2 mM thymidine for 18 h. In order to arrest HeLa or U2OS cells in mitosis, cells were first synchronized in G1/S phase by treatment with 2 mM thymidine for 17 h. The cells were released into the cell cycle by washing three times with PBS and incubation with fresh growth medium for 5 h. Finally, the cells were treated with 250 ng/ml nocodazole, 500-1000 nM Taxol, 500 nM vincristine, 5 µM STLC or 100 nM BI2536 for 16-17 h. Mitotic cells were collected by a mitotic shake-off.

MG132 and cycloheximide treatment

In order to inhibit proteasomal degradation in HEK-293T cells, the cells were treated with 10 µM MG132 (Sigma-Aldrich) for 4-5 h before harvesting. In order to inhibit protein synthesis in HeLa cells, they were treated with 100 µg/ml cycloheximide (Sigma-Aldrich). For a cycloheximide chase assay, the cells were harvested at different time points after cycloheximide treatment.

Live-cell imaging

For the analysis of mitotic cell fate or unperturbed mitotic progression, live-cell imaging was performed. For mitotic cell fate analysis, U2OS cells were transfected with 30 nM siRNA targeting GL2, FBXW7, FBXO45 or MYCBP2. 48 h after transfection, 2.5×10^4 cells were seeded into Ibidi dish chambers. 72 h after transfection, the cells were treated with 250 ng/ml nocodazole, 1 µM Taxol or 500 nM vincristine. 4 h after the spindle poison treatment, the cells were monitored by a 10x/0.3 EC PlnN Ph1 DICI objective on a Zeiss Cell Observer Z1 inverted microscope (AxioCam MRm camera system) with incubation at 5% CO_2 and 37°C. Multi-tile phase-contrast images were taken

every 10 min for 48 h using the Zeiss ZEN blue software. Data analysis was performed with ImageJ Fiji software. Cell death was defined by cell morphology and cessation of movement. Mitotic slippage was defined by mitotic exit without cell division. For the analysis of unperturbed mitotic progression, HeLa GFP-α-tubulin/RFP-H2B cells were transfected with 30 nM siRNA targeting GL2 or FBXO45 and MYCBP2. Analysis was performed as described previously (Kratz et al., 2016). 48 h after transfection, 2.5×10^4 cells were seeded into Ibidi dish chambers and arrested in G1/S phase by thymidine treatment. 24 h after thymidine addition, the cells were released from the arrest and analyzed by live-cell imaging using LED module Colibri.2 with 470 nm for GFP and 590 nm for RFP fluorochrome excitation.

Preparation of protein extracts from mammalian cells

For the preparation of cell extracts, cell pellets were resuspended in 3-5 volumes of RIPA, NP40 or Urea lysis buffer. RIPA lysis buffer (50 mM Tris-HCl pH 7.4, 1% NP40, 0.5% Na-deoxycholate, 0.1% SDS, 150 mM NaCl, 2 mM EDTA, 50 mM NaF, 1 mM DTT, 10 µg/ml TPCK, 5 µg/ml TLCK, 0.1 mM Na_3VO_4, 1 µg/ml Aprotinin, 1 µg/ml Leupeptin, 10 µg/ml Trypsin inhibitor from soybean) was used for the analysis of protein levels in whole cell extracts and for *in vivo* ubiquitylation assays. NP40 lysis buffer (40 mM Tris-HCl pH 7.5, 150 mM NaCl, 5 mM EDTA, 10 mM β-glycerophosphate, 5 mM NaF, 0.5% NP40, 1 mM DTT, 10 µg/ml TPCK, 5 µg/ml TLCK, 0.1 mM Na_3VO_4, 1 µg/ml Aprotinin, 1 µg/ml Leupeptin, 10 µg/ml Trypsin inhibitor from soybean) was used for immunoprecipitations. Urea lysis buffer (8 M Urea, 30 mM imidazole, 0.1 M phosphate buffer pH 8.0) was used for *in vivo* ubiquitylation assays. The cell lysates were incubated on ice for 30 min with short vortexing every 5-10 min. The lysates were cleared by centrifugation at maximal speed and 4°C in an Eppendorf 5415 R centrifuge for 15 min. The supernatants were transferred to fresh reaction tubes. Extracts of cytoplasmic and nuclear cell fractions were prepared using the CelLytic NuCLEAR Extraction Kit (Sigma) according to the manufacturer's instructions.

The protein concentration of a cell extract was determined according to the Bradford method in a Bio-Rad Protein assay. For SDS-PAGE, the cell extracts

were mixed with equal volumes of 2x Laemmli buffer and incubated at 95°C for 5 min.

Western blotting

The following antibodies were used for Western blotting: Rabbit α-FBXW7α antibody (A301-720A, 1:15000) was obtained from Bethyl. Rabbit α-FBXO45 (NBP1-91891, 1:500) was purchased from Novus. Rabbit α-MYCBP2 was a kind gift from K. Scholich (Dorr et al., 2015). Mouse α-Flag (M2, F3165, 1:5000), mouse α-tubulin (B-5-1-2, 1:10000) and mouse α-Vinculin (hVIN-1, 1:5000) were obtained from Sigma-Aldrich. Rabbit α-Cyclin B1 has been described before (Hoffmann et al., 1994). Mouse α-HA (16B12, 1:1000) was purchased from Babco. Mouse α-Myc (9E10, 1:500), rabbit α-SKP1 (H-163, 1:1000) and mouse α-ubiquitin (P4D1, 1:1000) were obtained from Santa Cruz. Mouse α-Nucleophosmin (NPM, 32-5200, 1:1000) was ordered from Zymed. Rabbit α-MCL-1 (4572, 1:1000) was obtained from Cell Signaling. Goat α-mouse IgG HRP (1:5000) was purchased from Novus. Donkey α-rabbit IgG HRP (1:5000) was obtained from Jackson Laboratories.

Immunoprecipitation

Immunoprecipitations of Flag-tagged proteins were performed using α-Flag M2 affinity beads (Sigma-Aldrich). For each immunoprecipitation reaction, 10-40 µl of the α-Flag M2 affinity bead suspension was used. The beads were washed twice with TBS, once with glycine buffer (0.1 M glycine-HCl pH 3.5) and three times with TBS. Buffers and beads were kept on ice and centrifugations were performed at 5000 rpm and 4°C for 2 min in an Eppendorf 5415 R centrifuge. HEK-293T or HeLa cell extracts were prepared with NP40 lysis buffer and 6-15 mg of each extract were transferred to the prepared beads. Each reaction was filled up to a final volume of 1 ml using NP40 lysis buffer. The reactions were incubated overnight on a rotating wheel at 4°C. After the incubation, the beads were washed 3-5 times with NP40 lysis buffer. Immunoprecipitated proteins were eluted from the beads by competition with 100 µl of a 3x Flag peptide solution (100-500 ng/µl in NP40 lysis buffer). The elution was carried out on ice for 30 min with short vortexing every 5-10 min. After the elution, the beads were centrifuged at 5000 rpm and

4°C for 2 min. 90 µl of the supernatant were transferred to a fresh reaction tube and 30 µl of 4x Laemmli buffer were added. After incubation at 95°C for 2 min, 20-40% of the immunoprecipitation sample were analyzed by SDS-PAGE and Western blotting.

In order to analyze whether proteins exist in ternary complexes, sequential immunoprecipitations were performed. In the first step of the experiment, 15-20 mg of HEK-293T cell extracts were used for an immunoprecipitation directed against a Flag-tagged MYCBP2 fragment. The immunoprecipitation was performed as described above. Instead of mixing the eluate with Laemmli buffer, it was used for a second immunoprecipitation directed against HA-FBXO45. HA-FBXO45 was immunoprecipitated with 20 µl of α-HA agarose beads (Sigma-Aldrich) according to the manufacturer's instructions. Finally, the beads were incubated with 30 µl of 2x Laemmli buffer at 95°C for 5 min. The supernatant was analyzed by SDS-PAGE and Western blotting.

Mass spectrometry analysis

Immunoprecipitation samples were analyzed by SDS-PAGE and stained by Colloidal Coomassie. Analysis was performed by M. Schnölzer (DKFZ Protein Analysis Facility, Heidelberg). Briefly, whole gel lanes were cut into slices. Proteins were reduced and alkylated by incubation with 10 mM DTT in 40 mM NH_4HCO_3 for 1 h at 56°C in the dark and incubation with 55 mM iodoacetamide in 40 mM NH_4HCO_3 for 30 min at 25°C. After washing of the slices with H_2O and 50% acetonitrile, they were dried with 100% acetonitrile. Proteins were digested in-gel with trypsin (0.17 µg in 10 µl 40 mM NH_4HCO_3, Promega) at 37°C over night. Tryptic peptides were extracted with 50% acetonitrile/0.1% TFA and 100% acetonitrile. Supernatants were lyophilized and redissolved in 0.1% TFA/5% hexafluoroisopropanol. Solutions were analyzed by nanoLC-ESI-MS/MS. Peptides were separated with a nanoAcquity UPLC system (Waters GmbH). Peptides were loaded on a C18 trap column with a particle size of 5 µm (Waters GmbH). Liquid chromatography was carried out on a BEH130 C18 column with a particle size of 1.7 µm (Waters GmbH). A 1 h gradient was applied for protein identification. The nanoUPLC system was connected to an LTQ Orbitrap XL mass spectrometer (Thermo Scientific). Data were acquired with the Xcalibur

476 software 2.1 (Thermo Scientific). The SwissProt database (taxonomy human)
477 was used for database searches with the MASCOT search engine (Matrix
478 Science). Data from individual gel slices were merged. Peptide mass
479 tolerance was 5 ppm, fragment mass tolerance was 0.4 Da and significance
480 threshold was $p<0.01$.
481
482 **_In vivo_ ubiquitylation assays**
483 HEK-293T cells transiently transfected with the indicated plasmids were
484 treated with 10 µM MG132 4-5 h before harvesting. Cells were harvested and
485 cell extracts were prepared with RIPA lysis buffer containing 10 mM of the
486 DUB inhibitor N-ethylmaleimide (NEM). 2-3 mg of protein extract were used
487 for each sample. Flag-FBXW7α was immunoprecipitated with α-Flag affinity
488 beads. Immunoprecipitation and washing steps were performed with RIPA
489 lysis buffer containing 10 mM NEM. Alternatively, endogenous FBXW7α was
490 immunoprecipitated by incubation of each protein extract with 1 µg of
491 FBXW7α antibody on a rotating wheel at 4°C overnight. After the incubation
492 with the antibody, the extracts were incubated with 15 µl of protein A
493 sepharose beads (GE Healthcare) on a rotating wheel at 4°C for 1 h. The
494 beads were washed four times with RIPA lysis buffer containing 10 mM NEM.
495 Finally, the beads were incubated in 30 µl of 2x Laemmli buffer at 95°C for
496 5 min. 25 µl of the supernatant were analyzed by SDS-PAGE and Western
497 blotting.
498 For denaturing ubiquitylation assays, cell extracts were prepared using Urea
499 lysis buffer. Cell extracts were sonified, centrifuged and incubated with Nickel-
500 NTA agarose beads on a rotating wheel at RT for 2 h. Afterwards, the beads
501 were washed four times with Urea lysis buffer and proteins were finally eluted
502 using 30 µl of 2x Laemmli buffer containing 200 mM imidazole. 25 µl of the
503 supernatant were analyzed by SDS-PAGE and Western blotting.
504
505 **Expression and purification of MBP-tagged proteins**
506 Chemically competent *E. coli* Rosetta (DE3) were transformed with pMAL-
507 MBP-FBXW7α-N167. A single colony was used to inoculate 10 ml of LB
508 medium containing 100 µg/ml ampicillin and 0.2% glucose. The culture was
509 incubated over night at 30°C with constant shaking at 180 rpm. The overnight

culture was used to inoculate 1 l of LB medium containing 100 µg/ml ampicillin and 0.2% glucose. The culture was incubated at 37°C with constant shaking at 180 rpm. When an OD_{600} of 0.5 was reached, the culture was cooled down on ice at 4°C and protein expression was induced by the addition of 0.4 mM isopropyl-β-D-thiogalactopyranoside (IPTG). The culture was further incubated over night at 18°C with constant shaking at 180 rpm. Bacteria were harvested by centrifugation at 5000 rpm and 4°C for 15 min (F10-6x500Y rotor, Piramoon). The pellet was resuspended in 25 ml of cold column buffer. Cell lysis was performed with a high pressure homogenizer (15000-17000 psi/1030-1170 bar for one pass, EmulsiFlex C5, Avestin). The lysate was centrifuged at 20000 g and 4°C for 20 min (WX Ultra 80, Thermo Scientific). The supernatant was applied onto a column with 1 ml of equilibrated amylose resin (NEB). The column with the beads and the extract was incubated on a rotating wheel at 4°C for 1 h. Afterwards, the beads were washed three times with 15 ml of column buffer. Finally, the proteins bound to the beads were eluted with 5 ml of column buffer containing 10 mM maltose. 10 fractions of 500 µl each were collected. Protein containing fractions were identified by spotting the fractions on nitrocellulose and staining with Ponceau S solution. Protein containing fractions were pooled and MBP-FBXW7α-N167 was further purified with a preparative Superdex 200 column in 50 mM Tris-HCl pH 8.0, 100 mM NaCl, 5 mM β-mercaptoethanol, 5% glycerol. Purified MBP-FBXW7α-N167 fractions were analyzed by SDS-PAGE and Colloidal Coomassie staining. Protein containing fractions were aliquoted, frozen in liquid nitrogen and stored at -80°C.

In vitro transcription and translation and *in vitro* binding assays

For *in vitro* binding assays, FBXO45 and MYCBP2(1951-2950) cDNA sequences in pCMV-3Tag1A backbones were transcribed and translated *in vitro* using the TNT T3 coupled reticulocyte system (Promega) according to the manufacturer's instructions. The proteins were synthesized in the presence of 20 µCi [^{35}S]-methionine so that synthesized proteins were radioactively labelled. 20 µl of the *in vitro* translated proteins were incubated with 10 µg of MBP-FBXW7α-N167 or MBP alone coupled to 10 µl of amylose beads in a final volume of 500 µl NP40 lysis buffer on a rotating wheel at 4°C

for 2 h. The beads were washed five times with 800 µl of NP40 lysis buffer. Finally, the beads were incubated with 30 µl of 2x Laemmli buffer at 95°C for 5 min. Input and pull-down samples were analyzed by SDS-PAGE and stained with Colloidal Coomassie. The gel was then incubated with Amersham Amplify Fluorographic reagent (GE Healthcare) for 30 min with gentle shaking. Afterwards, the gel was dried at 80°C for 1 h in a vacuum dryer and analyzed by autoradiography.

ACKNOWLEDGMENTS

We thank D. Gerlich, G. Melino, A. Peschiaroli and K. Scholich for providing reagents and cell lines. We acknowledge the DKFZ Mass Spectrometry and Microscopy Core Facilities for providing equipment and excellent technical assistance. We thank Bettina Dörr for expert technical assistance. We acknowledge the members of our lab for critically reading the manuscript.

AUTHOR CONTRIBUTION

IH and KTR designed the experiments. KTR, YTK and BV performed the experiments. IH and KTR wrote the paper.

DECLARATION OF INTERESTS

The authors declare no conflict of interests

REFERENCES

Allan, L.A., Skowyra, A., Rogers, K.I., Zeller, D., and Clarke, P.R. (2018). Atypical APC/C-dependent degradation of Mcl-1 provides an apoptotic timer during mitotic arrest. EMBO J *37*.

Balachandran, R.S., Heighington, C.S., Starostina, N.G., Anderson, J.W., Owen, D.L., Vasudevan, S., and Kipreos, E.T. (2016). The ubiquitin ligase CRL2ZYG11 targets cyclin B1 for degradation in a conserved pathway that facilitates mitotic slippage. J Cell Biol *215*, 151-166.

Brito, D.A., and Rieder, C.L. (2006). Mitotic checkpoint slippage in humans occurs via cyclin B destruction in the presence of an active checkpoint. Curr Biol *16*, 1194-1200.

Brito, D.A., Yang, Z., and Rieder, C.L. (2008). Microtubules do not promote mitotic slippage when the spindle assembly checkpoint cannot be satisfied. J Cell Biol *182*, 623-629.

582 Chen, X., Sahasrabuddhe, A.A., Szankasi, P., Chung, F., Basrur, V.,
583 Rangnekar, V.M., Pagano, M., Lim, M.S., and Elenitoba-Johnson, K.S.
584 (2014). Fbxo45-mediated degradation of the tumor-suppressor Par-4
585 regulates cancer cell survival. Cell Death Differ *21*, 1535-1545.
586 Cizmecioglu, O., Krause, A., Bahtz, R., Ehret, L., Malek, N., and Hoffmann, I.
587 (2012). Plk2 regulates centriole duplication through phosphorylation-mediated
588 degradation of Fbxw7 (human Cdc4). J Cell Sci *125*, 981-992.
589 Davis, R.J., Welcker, M., and Clurman, B.E. (2014). Tumor suppression by
590 the Fbw7 ubiquitin ligase: mechanisms and opportunities. Cancer Cell *26*,
591 455-464.
592 Dorr, A., Pierre, S., Zhang, D.D., Henke, M., Holland, S., and Scholich, K.
593 (2015). MYCBP2 Is a Guanosine Exchange Factor for Ran Protein and
594 Determines Its Localization in Neurons of Dorsal Root Ganglia. J Biol Chem
595 *290*, 25620-25635.
596 Duda, D.M., Olszewski, J.L., Tron, A.E., Hammel, M., Lambert, L.J., Waddell,
597 M.B., Mittag, T., DeCaprio, J.A., and Schulman, B.A. (2012). Structure of a
598 glomulin-RBX1-CUL1 complex: inhibition of a RING E3 ligase through
599 masking of its E2-binding surface. Mol Cell *47*, 371-382.
600 Ekholm-Reed, S., Goldberg, M.S., Schlossmacher, M.G., and Reed, S.I.
601 (2013). Parkin-dependent degradation of the F-box protein Fbw7beta
602 promotes neuronal survival in response to oxidative stress by stabilizing Mcl-
603 1. Mol Cell Biol *33*, 3627-3643.
604 Finkin, S., Aylon, Y., Anzi, S., Oren, M., and Shaulian, E. (2008). Fbw7
605 regulates the activity of endoreduplication mediators and the p53 pathway to
606 prevent drug-induced polyploidy. Oncogene *27*, 4411-4421.
607 Frederiks, C.N., Lam, S.W., Guchelaar, H.J., and Boven, E. (2015). Genetic
608 polymorphisms and paclitaxel- or docetaxel-induced toxicities: A systematic
609 review. Cancer Treat Rev *41*, 935-950.
610 Galan, J.M., and Peter, M. (1999). Ubiquitin-dependent degradation of
611 multiple F-box proteins by an autocatalytic mechanism. Proc Natl Acad Sci U
612 S A *96*, 9124-9129.
613 Gascoigne, K.E., and Taylor, S.S. (2008). Cancer cells display profound intra-
614 and interline variation following prolonged exposure to antimitotic drugs.
615 Cancer Cell *14*, 111-122.
616 Grill, B., Murphey, R.K., and Borgen, M.A. (2016). The PHR proteins:
617 intracellular signaling hubs in neuronal development and axon degeneration.
618 Neural Dev *11*, 8.
619 Gupta-Rossi, N., Le Bail, O., Gonen, H., Brou, C., Logeat, F., Six, E.,
620 Ciechanover, A., and Israel, A. (2001). Functional interaction between SEL-
621 10, an F-box protein, and the nuclear form of activated Notch1 receptor. J Biol
622 Chem *276*, 34371-34378.
623 Harley, M.E., Allan, L.A., Sanderson, H.S., and Clarke, P.R. (2010).
624 Phosphorylation of Mcl-1 by CDK1-cyclin B1 initiates its Cdc20-dependent
625 destruction during mitotic arrest. EMBO J *29*, 2407-2420.
626 Haschka, M., Karbon, G., Fava, L.L., and Villunger, A. (2018). Perturbing
627 mitosis for anti-cancer therapy: is cell death the only answer? EMBO Rep *19*.
628 Hershko, A., and Ciechanover, A. (1998). The ubiquitin system. Annu Rev
629 Biochem *67*, 425-479.

Hoffmann, I., Draetta, G., and Karsenti, E. (1994). Activation of the phosphatase activity of human cdc25A by a cdk2-cyclin E dependent phosphorylation at the G1/S transition. EMBO J *13*, 4302-4310.

Hubbard, E.J., Wu, G., Kitajewski, J., and Greenwald, I. (1997). sel-10, a negative regulator of lin-12 activity in Caenorhabditis elegans, encodes a member of the CDC4 family of proteins. Genes Dev *11*, 3182-3193.

Huttlin, E.L., Bruckner, R.J., Paulo, J.A., Cannon, J.R., Ting, L., Baltier, K., Colby, G., Gebreab, F., Gygi, M.P., Parzen, H.*, et al.* (2017). Architecture of the human interactome defines protein communities and disease networks. Nature *545*, 505-509.

Kimura, T., Gotoh, M., Nakamura, Y., and Arakawa, H. (2003). hCDC4b, a regulator of cyclin E, as a direct transcriptional target of p53. Cancer Sci *94*, 431-436.

Koepp, D.M., Schaefer, L.K., Ye, X., Keyomarsi, K., Chu, C., Harper, J.W., and Elledge, S.J. (2001). Phosphorylation-dependent ubiquitination of cyclin E by the SCFFbw7 ubiquitin ligase. Science *294*, 173-177.

Kourtis, N., Moubarak, R.S., Aranda-Orgilles, B., Lui, K., Aydin, I.T., Trimarchi, T., Darvishian, F., Salvaggio, C., Zhong, J., Bhatt, K.*, et al.* (2015). FBXW7 modulates cellular stress response and metastatic potential through HSF1 post-translational modification. Nat Cell Biol *17*, 322-332.

Kratz, A.S., Richter, K.T., Schlosser, Y.T., Schmitt, M., Shumilov, A., Delecluse, H.J., and Hoffmann, I. (2016). Fbxo28 promotes mitotic progression and regulates topoisomerase IIalpha-dependent DNA decatenation. Cell Cycle *15*, 3419-3431.

Kugler, J.M., Woo, J.S., Oh, B.H., and Lasko, P. (2010). Regulation of Drosophila vasa in vivo through paralogous cullin-RING E3 ligase specificity receptors. Mol Cell Biol *30*, 1769-1782.

Liao, E.H., Hung, W., Abrams, B., and Zhen, M. (2004). An SCF-like ubiquitin ligase complex that controls presynaptic differentiation. Nature *430*, 345-350.

Moberg, K.H., Bell, D.W., Wahrer, D.C., Haber, D.A., and Hariharan, I.K. (2001). Archipelago regulates Cyclin E levels in Drosophila and is mutated in human cancer cell lines. Nature *413*, 311-316.

Nakata, K., Abrams, B., Grill, B., Goncharov, A., Huang, X., Chisholm, A.D., and Jin, Y. (2005). Regulation of a DLK-1 and p38 MAP kinase pathway by the ubiquitin ligase RPM-1 is required for presynaptic development. Cell *120*, 407-420.

Nateri, A.S., Riera-Sans, L., Da Costa, C., and Behrens, A. (2004). The ubiquitin ligase SCFFbw7 antagonizes apoptotic JNK signaling. Science *303*, 1374-1378.

Pao, K.C., Wood, N.T., Knebel, A., Rafie, K., Stanley, M., Mabbitt, P.D., Sundaramoorthy, R., Hofmann, K., van Aalten, D.M.F., and Virdee, S. (2018). Activity-based E3 ligase profiling uncovers an E3 ligase with esterification activity. Nature *556*, 381-385.

Pierre, S.C., Hausler, J., Birod, K., Geisslinger, G., and Scholich, K. (2004). PAM mediates sustained inhibition of cAMP signaling by sphingosine-1-phosphate. EMBO J *23*, 3031-3040.

Po, M.D., Hwang, C., and Zhen, M. (2010). PHRs: bridging axon guidance, outgrowth and synapse development. Curr Opin Neurobiol *20*, 100-107.

Rieder, C.L., and Maiato, H. (2004). Stuck in division or passing through: what happens when cells cannot satisfy the spindle assembly checkpoint. Dev Cell *7*, 637-651.

Sloss, O., Topham, C., Diez, M., and Taylor, S. (2016). Mcl-1 dynamics influence mitotic slippage and death in mitosis. Oncotarget *7*, 5176-5192.

Strohmaier, H., Spruck, C.H., Kaiser, P., Won, K.A., Sangfelt, O., and Reed, S.I. (2001). Human F-box protein hCdc4 targets cyclin E for proteolysis and is mutated in a breast cancer cell line. Nature *413*, 316-322.

Tron, A.E., Arai, T., Duda, D.M., Kuwabara, H., Olszewski, J.L., Fujiwara, Y., Bahamon, B.N., Signoretti, S., Schulman, B.A., and DeCaprio, J.A. (2012). The glomuvenous malformation protein Glomulin binds Rbx1 and regulates cullin RING ligase-mediated turnover of Fbw7. Mol Cell *46*, 67-78.

Wei, W., Jin, J., Schlisio, S., Harper, J.W., and Kaelin, W.G., Jr. (2005). The v-Jun point mutation allows c-Jun to escape GSK3-dependent recognition and destruction by the Fbw7 ubiquitin ligase. Cancer Cell *8*, 25-33.

Welcker, M., and Clurman, B.E. (2008). FBW7 ubiquitin ligase: a tumour suppressor at the crossroads of cell division, growth and differentiation. Nat Rev Cancer *8*, 83-93.

Welcker, M., Orian, A., Jin, J., Grim, J.E., Harper, J.W., Eisenman, R.N., and Clurman, B.E. (2004). The Fbw7 tumor suppressor regulates glycogen synthase kinase 3 phosphorylation-dependent c-Myc protein degradation. Proc Natl Acad Sci U S A *101*, 9085-9090.

Wertz, I.E., Kusam, S., Lam, C., Okamoto, T., Sandoval, W., Anderson, D.J., Helgason, E., Ernst, J.A., Eby, M., Liu, J.*, et al.* (2011). Sensitivity to antitubulin chemotherapeutics is regulated by MCL1 and FBW7. Nature *471*, 110-114.

Xiong, X., Hao, Y., Sun, K., Li, J., Li, X., Mishra, B., Soppina, P., Wu, C., Hume, R.I., and Collins, C.A. (2012). The Highwire ubiquitin ligase promotes axonal degeneration by tuning levels of Nmnat protein. PLoS Biol *10*, e1001440.

Yada, M., Hatakeyama, S., Kamura, T., Nishiyama, M., Tsunematsu, R., Imaki, H., Ishida, N., Okumura, F., Nakayama, K., and Nakayama, K.I. (2004). Phosphorylation-dependent degradation of c-Myc is mediated by the F-box protein Fbw7. EMBO J *23*, 2116-2125.

Figure 1. FBXO45-MYCBP2 binds to a conserved N-terminal motif of FBXW7α

(A) FBXW7α protein levels decrease during prolonged mitotic arrest. HeLa cells were treated with 250 ng/ml nocodazole for 2 h. Mitotic cells were collected by mitotic shake-off (time point 0) and further incubated with 250 ng/ml nocodazole. The cells were harvested at different time points by a mitotic shake-off. (Left) Cell extracts were prepared and analyzed by Western blotting. (Middle) Relative FBXW7α signal intensities were quantified. Average signal intensities and standard deviations from n=4 experiments were calculated. Statistical significance (difference to time point 0) was analyzed by a two-tailed, unpaired t-test with unequal variance. * $p<0.05$; ** $p<0.01$. (Right) Mitotic arrest was confirmed for two time points (0 h and 8 h) by FACS analysis. Asynchronous (asy.) cells served as a control.

(B) Flag-FBXO45 interacts with endogenous FBXW7α. Flag-FBXO45 was overexpressed in HEK-293T cells for 24 h. Cell extracts were used for an immunoprecipitation directed against the Flag tag.

(C) (Top) Schematic representation of Δ106-126 deletion in FBXW7α used in immunoprecipitation experiments. Positions of N-terminal domain (blue), dimerization domain (green), F-box domain (yellow) and WD40 domain (red) are indicated. (Bottom) FBXO45 and MYCBP2 interact with the N-terminal domain of FBXW7α. Flag-FBXW7α FL or Flag-FBXW7αΔ106-126 were overexpressed in HEK-293T cells for 24 h. Cell extracts were used for α-Flag immunoprecipitations.

(D) Sequence alignment of amino acid residues 106-126 from human FBXW7α with homologues from *Macaca mulatta, Mus musculus, Xenopus laevis* and *Danio rerio*.

(E) Either MBP alone or MBP-FBXW7α-N167 were incubated with *in vitro* translated and [^{35}S]-methionine containing FBXO45 or MYCBP2(1951-2950). MBP was pulled down with amylose beads. Pull-down samples were analyzed by SDS-PAGE and Colloidal Coomassie staining. *In vitro* translated proteins were detected by autoradiography.

(F) FBXW7α forms a complex with MYCBP2 and FBXO45. Flag-MYCBP2(1951-2950) and HA-FBXO45 were co-expressed in HEK-293T cells for 24 h. Cell extracts were used for an immunoprecipitation with α-Flag

agarose beads. Immunoprecipitated proteins were eluted by competition with Flag peptide. Eluates were used for a second immunoprecipitation directed against the HA tag. Immunoprecipitates obtained after sequential immunoprecipitation were analyzed by Western blotting.

Figure 2. FBXO45 and MYCBP2 downregulate FBXW7α protein levels during mitotic arrest

(A) FBXW7α is a nuclear protein, whereas FBXO45 is localized in the cytoplasm. Cytoplasmic and nuclear extracts were prepared from HeLa cells and analyzed by Western blotting.

(B) FBXO45 and FBXW7α interact predominantly in mitosis. Flag-FBXO45 was overexpressed in HeLa cells. Asynchronous or mitotic cells that had been treated with nocodazole for 17 h were harvested. Cytoplasmic extracts were used for an immunoprecipitation directed against the Flag tag.

(C) HeLa cells were transfected with 30 nM FBXO45 or FBXW7 siRNAs for 72 h. GL2 siRNA was used as a control. The cells were arrested in mitosis by nocodazole (noco.) treatment for 17 h and collected by a mitotic shake-off. Mitotic cells were compared with an asynchronous (asy.) cell population. (Top) Cell extracts were analyzed by Western blotting. Crossreacting band in FBXO45 immunoblot is marked with an asterisk. As the samples were analyzed in three Western blots, three vinculin immunoblots are shown as loading controls. (Bottom) Quantification of relative FBXW7α and FBXO45 signal intensities are shown. Relative FBXW7α and FBXO45 signals in the GL2 controls were set to 1. Average signal intensities and standard deviations from n=4 experiments were calculated. Statistical significance was analyzed by a two-tailed, unpaired t-test with unequal variance. * $p<0.05$; n.s.: not significant.

(D) Expression of Flag-MYCBP2(1951-2950) was induced in a stable U2OS Flp-In-T-Rex cell line by doxycycline treatment. The cells were arrested in mitosis by nocodazole treatment (noco.). Alternatively, they were treated with thymidine (thym.) or left untreated (asy.). U2OS cells that do not express the MYCBP2 fragment served as controls. (Top) Cell extracts were analyzed by Western blotting. Crossreacting band in Flag immunoblot is marked with an asterisk. (Bottom) Quantification of relative FBXW7α signal intensity was performed as described in (C).

Figure 3. FBXO45 and MYCBP2 promote the ubiquitylation and destabilization of FBXW7α

(A) Myc-FBXO45 and HA-Ubiquitin or Myc-MYCBP2 and Flag-FBXW7α were overexpressed in HEK-293T cells for 48 h. Cells were arrested in mitotis by nocodazole treatment for 17 h. 4 h before harvesting, cells were treated with MG132. Cell extracts were used for immunoprecipitations directed against endogenous FBXW7α or against the Flag tag.

(B) Flag-FBXW7α FL or Flag-FBXW7αΔ106-126 were co-expressed with His-Ubiquitin in HEK-293T cells. The cells were arrested in mitosis by nocodazole treatment. 4 h before harvesting, cells were treated with MG132. Cell extracts were prepared and α-His pull-downs were performed.

(C) HeLa cells were transfected with 30 nM of GL2 or FBXO45 siRNA for 72 h. 17 h before harvesting, the cells were treated with nocodazole. Mitotic cells were collected by mitotic shake-off and further incubated with nocodazole and cycloheximide (CHX). The cells were harvested at different time points after the addition of cycloheximide by mitotic shake-off. Cell extracts were analyzed by Western blotting. Relative FBXW7α signal intensities were quantified.

(D) Flag-FBXW7α FL or Flag-FBXW7αΔ106-126 were overexpressed in U2OS Flp-In-T-Rex cells by treatment with doxycycline. Cells were arrested in mitosis by nocodazole treatment. Cycloheximide (CHX) was added and cells were harvested at different time points after the addition of cycloheximide. MG132 was added in order to inhibit the proteasome. Cell extracts were analyzed by Western blotting. Relative Flag signal intensities were quantified.

Figure 4. FBXO45 and MYCBP2 cause mitotic slippage

(A) U2OS cells were transfected with 30 nM of GL2 or different FBXO45 siRNAs for 48 h and further incubated with 250 ng/mL nocodazole. Percentages of cells undergoing mitotic cell death were quantified. Cells from n=3 independent experiments were analyzed. In each experiment, 50 cells were quantified.

(B) U2OS cells were cotransfected with 40 nM of GL2 or FBXO45 siRNA and an empty vector (EV) or an siRNA resistant version of Flag-FBXO45. 48 h after transfection, the cells were treated with nocodazole and mitotic cell fate was analyzed by live-cell imaging. Cells from n=4 independent experiments were quantified.

(C) Expression of Flag-MYCBP2(1951-2950) was induced in U2OS cells by treatment with doxycycline for 48 h. Cells were arrested in mitosis by treatment with nocodazole and mitotic cell fate was analyzed by live-cell imaging. Cells from n=3 independent experiments were analyzed.

(D) U2OS cells were transfected with 30 nM of GL2 or FBXO45 siRNA for 48 h and further incubated with 1 µM Taxol for 24 h, 48 h or 72 h. DNA content was analyzed by FACS.

(E) U2OS cells were transfected with 30 nM of GL2, FBXO45 or FBXW7 siRNA or co-transfected with FBXO45 and FBXW7 siRNA. 48 h after transfection, the cells were treated with nocodazole and mitotic cell fate was analyzed by live-cell imaging. Cells from n=3 independent experiments were quantified.

For statistical analysis in (A)-(E), significance was analyzed by a two-tailed, unpaired t-test. * $p<0.05$, ** $p<0.01$, n.s.: not significant.

Table S1. Identification of FBXW7α interaction partners

Selection of proteins that were specifically identified in co-immunoprecipitation with Flag-FBXW7α. For each protein, the MASCOT score, mass, number of significant sequences and coverage are specified.

Protein name	Score	Mass	Sign. Sequences	Coverage (%)
MYCBP2	12344	517856	164	50.3
CUL1	4091	90334	59	73.2
FBXW7	3143	80583	42	71.9
SKP1	1059	18817	12	95.7
FBXO45	908	31183	13	43.4
MYC	789	49344	9	26.2
NOTCH2	375	279081	4	4.3
MED13L	142	210603	1	2.6
NEDD8	116	8555	2	30.3
NOTCH1	97	274439	1	0.7
ARIH1	76	31920	1	6.5
RBX1	72	12722	1	13
AURORA-B	62	39977	0	6.3
MED13	56	242728	0	0.9
MTOR	50	158783	0	1.1

Figure S1: Related to Figure 1

(A) Decrease in FBXW7α protein levels during prolonged mitotic arrest depends on proteasomal activity. HeLa cells were treated with 250 ng/ml nocodazole for 2 h. Mitotic cells were collected by mitotic shake-off (time point 0) and further incubated with 250 ng/ml nocodazole. MG132 was added in order to inhibit the proteasome. Cells were harvested at different time points by a mitotic shake-off. Cell extracts were prepared and analyzed by Western blotting. Relative FBXW7α, Cyclin B1 and MCL-1 signal intensities were quantified.

(B-C) The indicated Flag-tagged versions of FBXW7α were overexpressed in HEK-293T cells for 24 h. Cell extracts were used for immunoprecipitations with α-Flag agarose beads.

(D) Overview of Flag-tagged FBXW7α fragments used in (A-B). Positions of N-terminal domain (blue), dimerization domain (green), F-box domain (yellow) and WD40 domain (red) are indicated.

(E) FBXO45 specifically interacts with the α-isoform of FBXW7. Flag-FBXW7α, Flag-FBXW7β or Flag-FBXW7γ were overexpressed in HEK-293T cells for 24 h. FBXW7 isoforms were immunoprecipitated by their Flag tags. Immunoprecipitates were analyzed by Western blotting.

(F) Overview of MYCBP2 fragments used in (F). Positions of RCC1-like domain (blue), PHR domains (green), MYC-binding domain (yellow) and RING domain (red) are shown.

(G) FBXW7α and FBXO45 interact with the central domain of MYCBP2. The indicated Flag-tagged MYCBP2 fragments were overexpressed in HEK-293T cells for 24 h. Cell extracts were used for α-Flag immunoprecipitations.

Figure S2: Related to Figure 2

(A) HeLa cells were transfected with 30 nM FBXO45 and MYCBP2 siRNAs for 72 h. GL2 siRNA was used as a control. The cells were arrested in mitosis by nocodazole (noco.) treatment for 17 h and collected by a mitotic shake-off. Alternatively, mitotic cells were enriched after a release from a double-thymidine block (thym. release), followed by a mitotic shake-off when the cells reached the mitotic peak. Mitotic cells were compared with an asynchronous (asy.) cell population. (Top) Cell extracts were analyzed by Western blotting. (Bottom) A quantification of relative FBXW7α signal intensities is shown. Relative FBXW7α signals in the GL2 controls were set to 1. Average signal intensities and standard deviations from n=5 experiments were calculated. Statistical significance was analyzed by a two-tailed, unpaired t-test with unequal variance. * $p<0.05$; n.s.: not significant.

(B) Characterization of MYCBP2 siRNAs used in this study. HeLa cells were transfected with 30 nM of GL2 or MYCBP2 siRNAs for 72 h. Cell extracts were analyzed by Western blotting.

(C) HeLa cells were transfected with 30 nM of GL2 siRNA, three different FBXO45 siRNAs or two different MYCBP2 siRNAs for 72 h. In addition, the cells were treated with nocodazole for 17 h before they were collected by a mitotic shake-off. (Top) Cell extracts were analyzed by Western blotting. (Bottom) Relative FBXW7α signal intensities were quantified. Relative signal intensity in the GL2 control was set to 1. Average signal intensities and standard deviations from n=3 experiments were calculated. Statistical significance was analyzed by a two-tailed, unpaired t-test with unequal variance. * $p<0.05$; ** $p<0.01$.

(D) U2OS cells were transfected with 30 nM of GL2 or FBXO45 siRNA for 72 h. 17 h before harvesting, they were arrested in mitosis by treatment with nocodazole. Mitotic cells were harvested by mitotic shake-off. Cell extracts were analyzed by Western blotting.

(E-I) HeLa cells were transfected with 30 nM of GL2 or FBXO45 siRNA for 72 h. 17 h before harvesting, they were arrested in mitosis by treatment with nocodazole (noco., (E)), Taxol (F), vincristine (vincr., (G)), STLC (H) or BI2536 (I). Mitotic cells were harvested by mitotic shake-off. Cell extracts

were prepared and analyzed by Western blotting. Relative FBXW7α signal intensities were quantified.

Figure S3: Related to Figure 4

(A) U2OS cells were treated with 250 ng/mL nocodazole. 4 h after nocodazole addition, cells were analyzed by live-cell imaging. Representative images from live-cell imaging are shown. Time point 0 marks induction of mitotic cell death or mitotic slippage. Scale bars: 20 µm.

(B) U2OS cells were transfected with 30 nM of GL2 or FBXO45 siRNA for 48 h and further incubated with 1 µM Taxol. Percentages of cells undergoing mitotic cell death were quantified. Cells from n=4 independent experiments were analyzed. In each experiment, 50 cells were quantified. Statistical significance was analyzed by a two-tailed, unpaired t-test. * $p<0.05$.

(C) U2OS cells were transfected with 30 nM of GL2 or FBXO45 siRNA for 48 h and further incubated with 1 µM vincristine. Percentages of cells undergoing mitotic cell death were quantified. Cells from n=4 independent experiments were analyzed. In each experiment, 50 cells were quantified. Statistical significance was analyzed by a two-tailed, unpaired t-test. * $p<0.05$.

(D) U2OS cells were transfected with 30 nM of GL2 or two different MYCBP2 siRNAs for 48 h and further incubated with 250 ng/mL nocodazole. Percentages of cells undergoing mitotic cell death were quantified. Cells from n=4 independent experiments were analyzed. In each experiment, 50 cells were quantified. Statistical significance was analyzed by a two-tailed, unpaired t-test. * $p<0.05$.

(E) HeLa H2B-RFP/GFP-α-tubulin cells were transfected with 30 nM of GL2 or FBXO45/MYCBP2 siRNAs for 72 h. They were released from a thymidine block and their mitotic progression was analyzed and quantified by live-cell imaging.

(F) HeLa cells were transfected with 30 nM of GL2 or FBXO45 siRNA for 48 h and further incubated with nocodazole for 24 h, 48 h or 72 h. DNA content was analyzed by FACS.

Video S1: Related to Figure 4

Exemplary video of a U2OS cell undergoing mitotic cell death upon prolonged mitotic arrest. Mitotic arrest was caused by treatment with nocodazole.

Video S2: Related to Figure 4

Exemplary video of a U2OS cell undergoing mitotic slippage upon prolonged mitotic arrest. Mitotic arrest was caused by treatment with nocodazole.

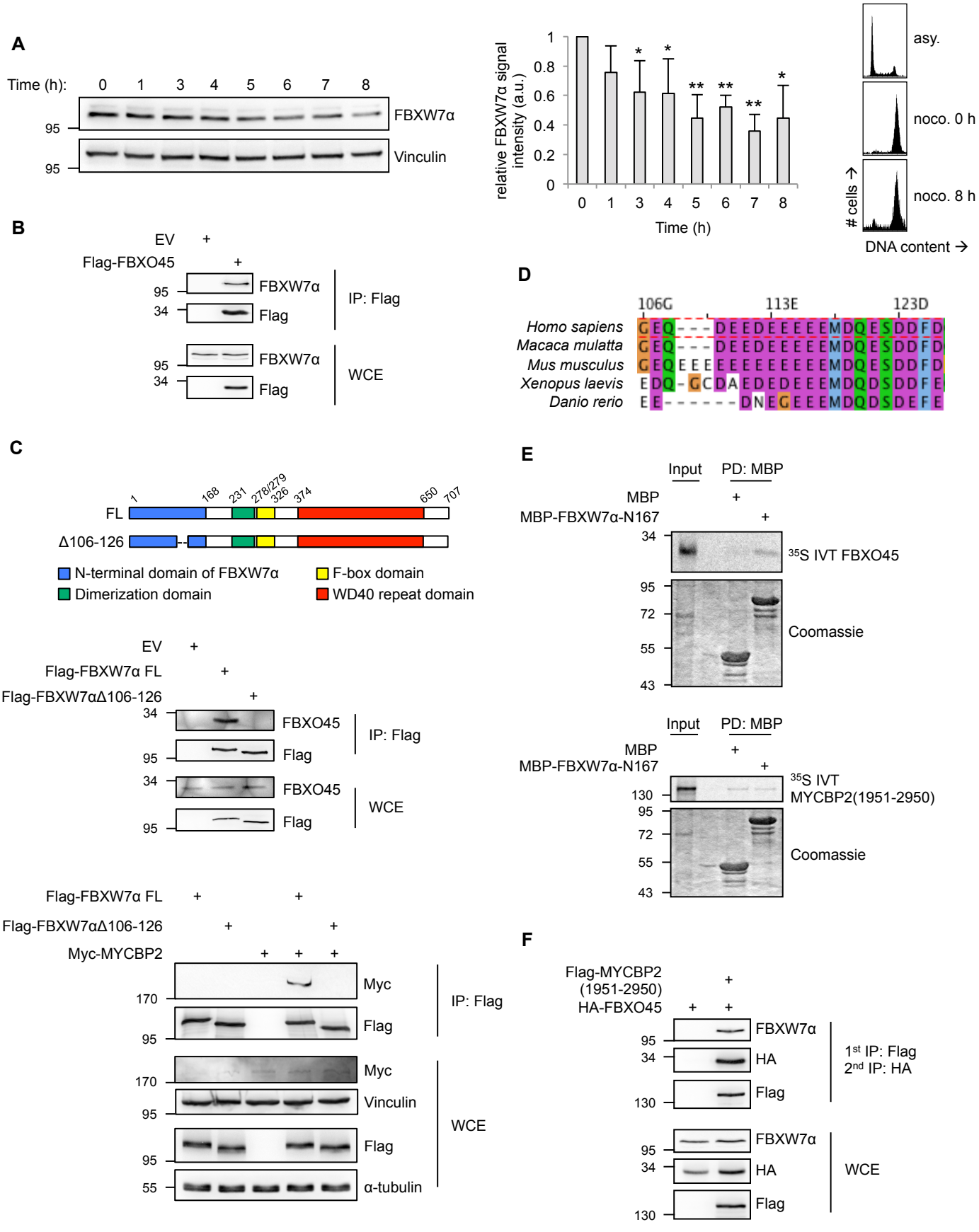
A
Time (h): 0 1 3 4 5 6 7 8
95
FBXW7α
95
Vinculin
relative FBXW7α signal intensity (a.u.)
1
0.8
0.6
0.4
0.2
0
0 1 3 4 5 6 7 8
Time (h)
asy.
noco. 0 h
noco. 8 h
cells →
DNA content →
B
EV +
Flag-FBXO45 +
95
FBXW7α
34
Flag
IP: Flag
95
FBXW7α
34
Flag
WCE
D
106G
113E
123D
Homo sapiens
Macaca mulatta
Mus musculus
Xenopus laevis
Danio rerio
C
1
168
231
278/279
326
374
650
707
FL
Δ106-126
N-terminal domain of FBXW7α
F-box domain
Dimerization domain
WD40 repeat domain
EV +
Flag-FBXW7α FL +
Flag-FBXW7αΔ106-126 +
34
FBXO45
95
Flag
IP: Flag
34
FBXO45
95
Flag
WCE
E
Input
PD: MBP
MBP +
MBP-FBXW7α-N167 +
34
35S IVT FBXO45
95
72
55
43
Coomassie
Input
PD: MBP
MBP +
MBP-FBXW7α-N167 +
130
95
35S IVT
MYCBP2(1951-2950)
72
55
43
Coomassie
F
Flag-FBXW7α FL + +
Flag-FBXW7αΔ106-126 + +
Myc-MYCBP2 + + +
170
Myc
95
Flag
IP: Flag
170
Myc
Vinculin
95
Flag
95
α-tubulin
55
WCE
Flag-MYCBP2 (1951-2950) +
HA-FBXO45 + +
95
FBXW7α
34
HA
130
Flag
1st IP: Flag
2nd IP: HA
95
FBXW7α
34
HA
130
Flag
WCE

Figure 1

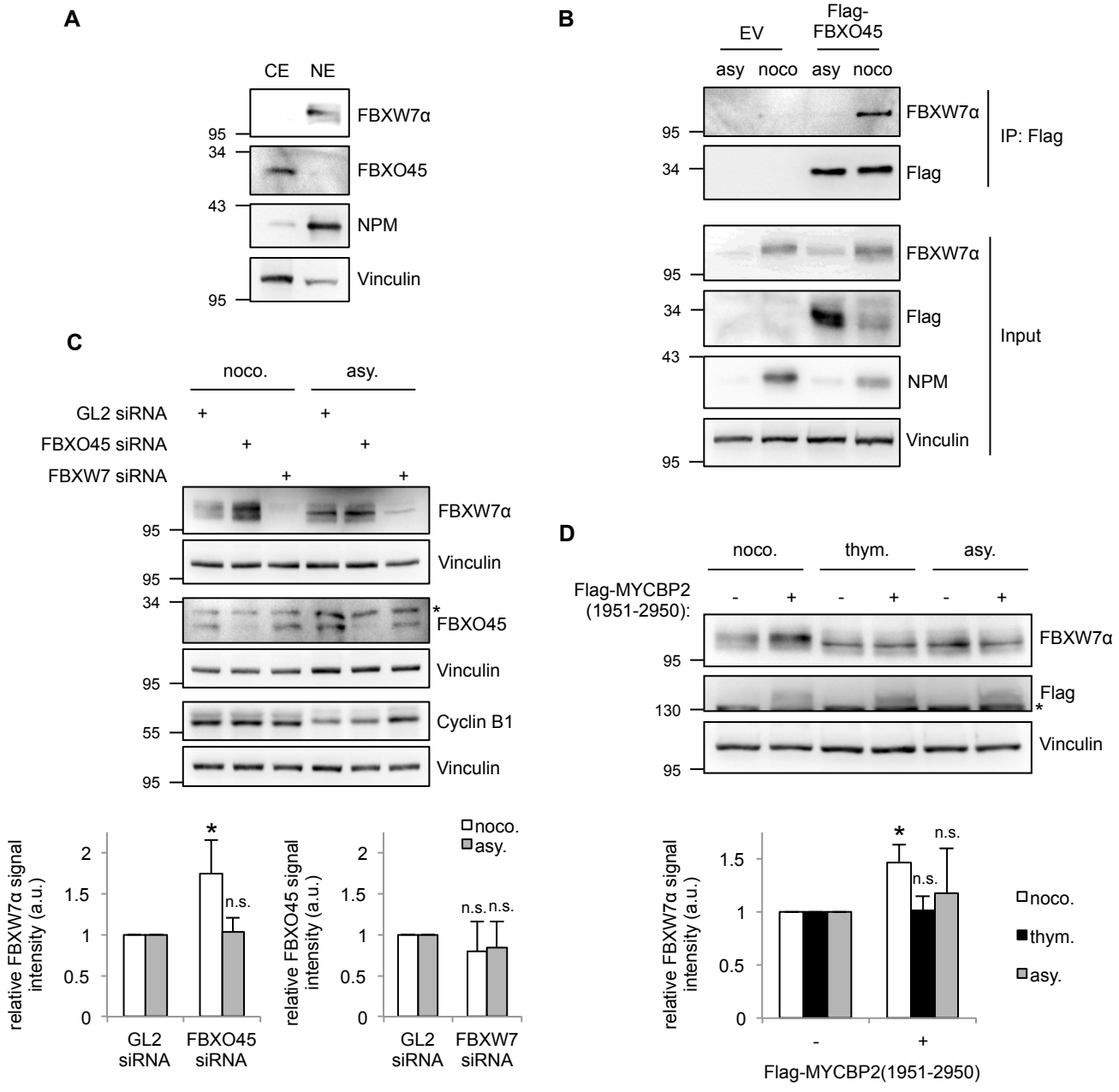
A
CE
NE
FBXW7α
FBXO45
NPM
Vinculin
95
34
43
95
B
EV
Flag-FBXO45
asy
noco
asy
noco
FBXW7α
Flag
IP: Flag
Input
NPM
Vinculin
C
noco.
asy.
GL2 siRNA
FBXO45 siRNA
FBXW7 siRNA
FBXW7α
Vinculin
FBXO45
Cyclin B1
relative FBXW7α signal intensity (a.u.)
relative FBXO45 signal intensity (a.u.)
n.s.
GL2 siRNA
FBXO45 siRNA
FBXW7 siRNA
D
noco.
thym.
asy.
Flag-MYCBP2 (1951-2950):
Flag
Flag-MYCBP2(1951-2950)

Figure 2

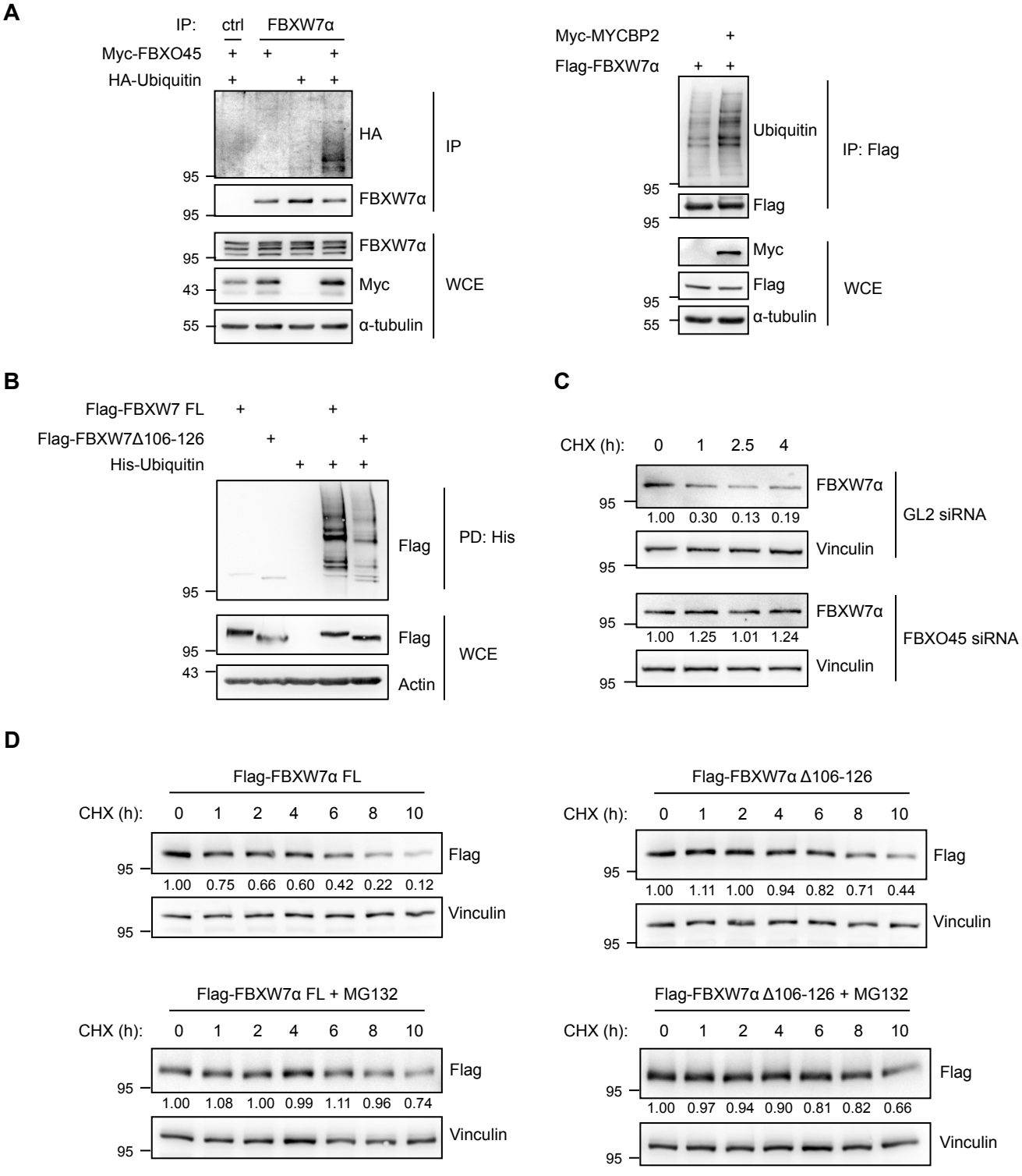
A
IP: ctrl FBXW7α
Myc-FBXO45 + + +
HA-Ubiquitin + + +
HA
IP
95
FBXW7α
95
FBXW7α
95
Myc
43
α-tubulin
55
WCE
Myc-MYCBP2 +
Flag-FBXW7α + +
Ubiquitin
IP: Flag
95
Flag
95
Myc
Flag
95
α-tubulin
55
WCE
B
Flag-FBXW7 FL + +
Flag-FBXW7Δ106-126 + +
His-Ubiquitin + + +
Flag
PD: His
95
Flag
95
Actin
43
WCE
C
CHX (h): 0 1 2.5 4
95
FBXW7α
1.00 0.30 0.13 0.19
GL2 siRNA
Vinculin
95
95
FBXW7α
1.00 1.25 1.01 1.24
FBXO45 siRNA
Vinculin
95
D
Flag-FBXW7α FL
CHX (h): 0 1 2 4 6 8 10
95
Flag
1.00 0.75 0.66 0.60 0.42 0.22 0.12
95
Vinculin
Flag-FBXW7α Δ106-126
CHX (h): 0 1 2 4 6 8 10
95
Flag
1.00 1.11 1.00 0.94 0.82 0.71 0.44
95
Vinculin
Flag-FBXW7α FL + MG132
CHX (h): 0 1 2 4 6 8 10
95
Flag
1.00 1.08 1.00 0.99 1.11 0.96 0.74
95
Vinculin
Flag-FBXW7α Δ106-126 + MG132
CHX (h): 0 1 2 4 6 8 10
95
Flag
1.00 0.97 0.94 0.90 0.81 0.82 0.66
95
Vinculin

Figure 3

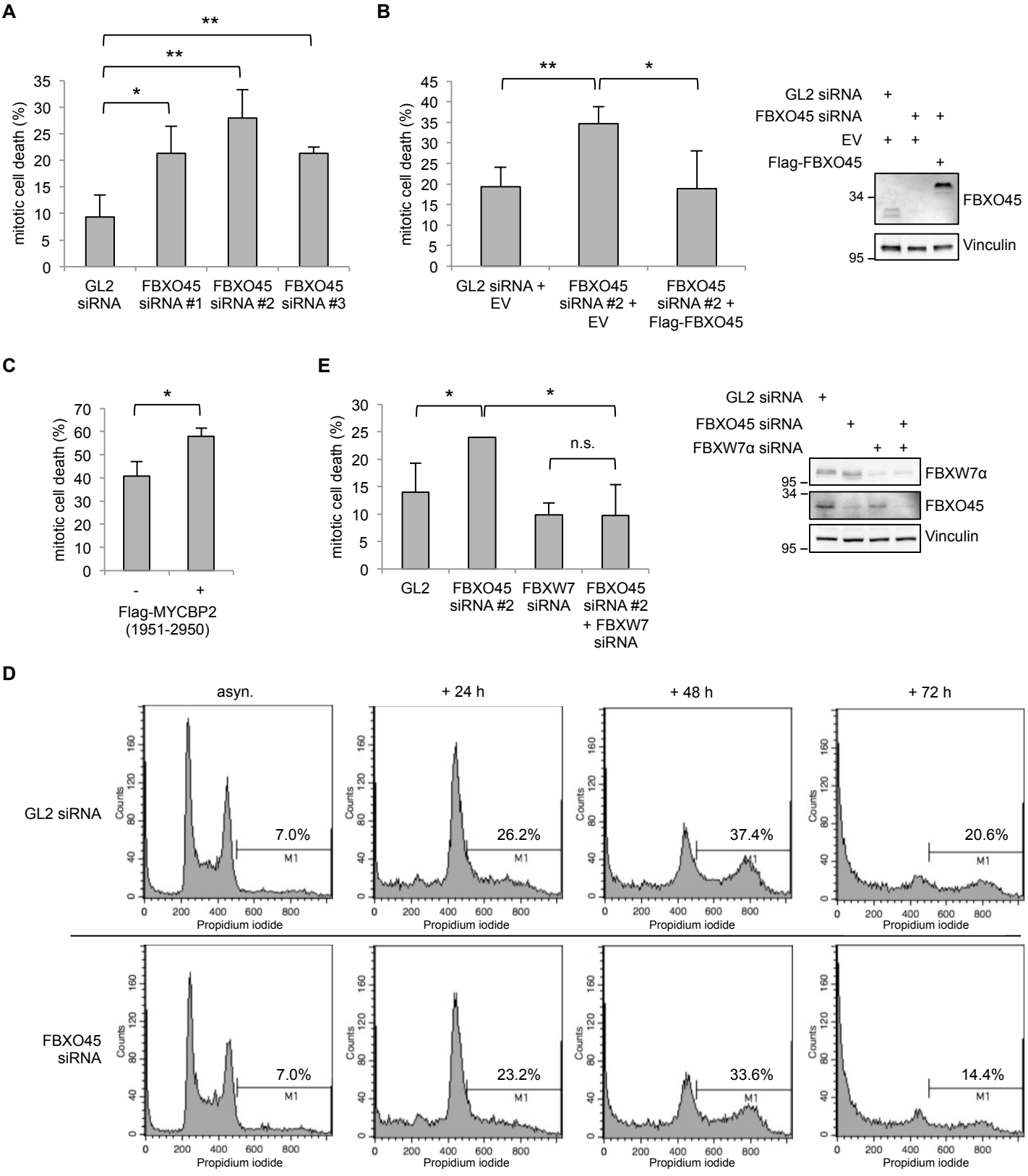
A
mitotic cell death (%)
GL2 siRNA
FBXO45 siRNA #1
FBXO45 siRNA #2
FBXO45 siRNA #3
B
mitotic cell death (%)
GL2 siRNA + EV
FBXO45 siRNA #2 + EV
FBXO45 siRNA #2 + Flag-FBXO45
GL2 siRNA
FBXO45 siRNA
EV
Flag-FBXO45
34
FBXO45
95
Vinculin
C
mitotic cell death (%)
Flag-MYCBP2 (1951-2950)
E
mitotic cell death (%)
n.s.
GL2
FBXO45 siRNA #2
FBXW7 siRNA
FBXO45 siRNA #2 + FBXW7 siRNA
GL2 siRNA
FBXO45 siRNA
FBXW7α siRNA
95
34
FBXW7α
FBXO45
Vinculin
95
D
asyn.
+ 24 h
+ 48 h
+ 72 h
GL2 siRNA
FBXO45 siRNA
Counts
Propidium iodide
M1
7.0%
26.2%
37.4%
20.6%
7.0%
23.2%
33.6%
14.4%

Figure 4

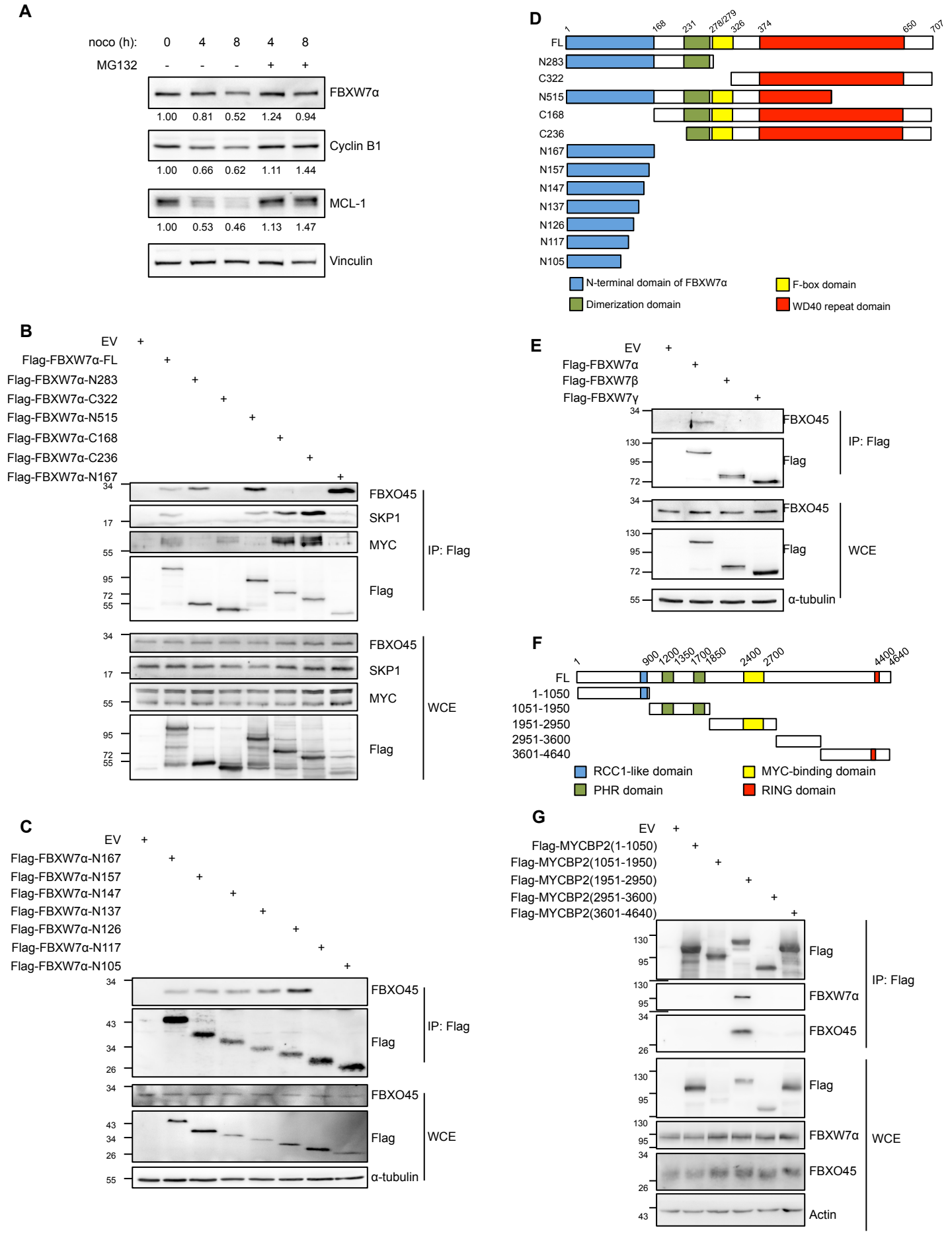

Figure S1: Related to Figure 1

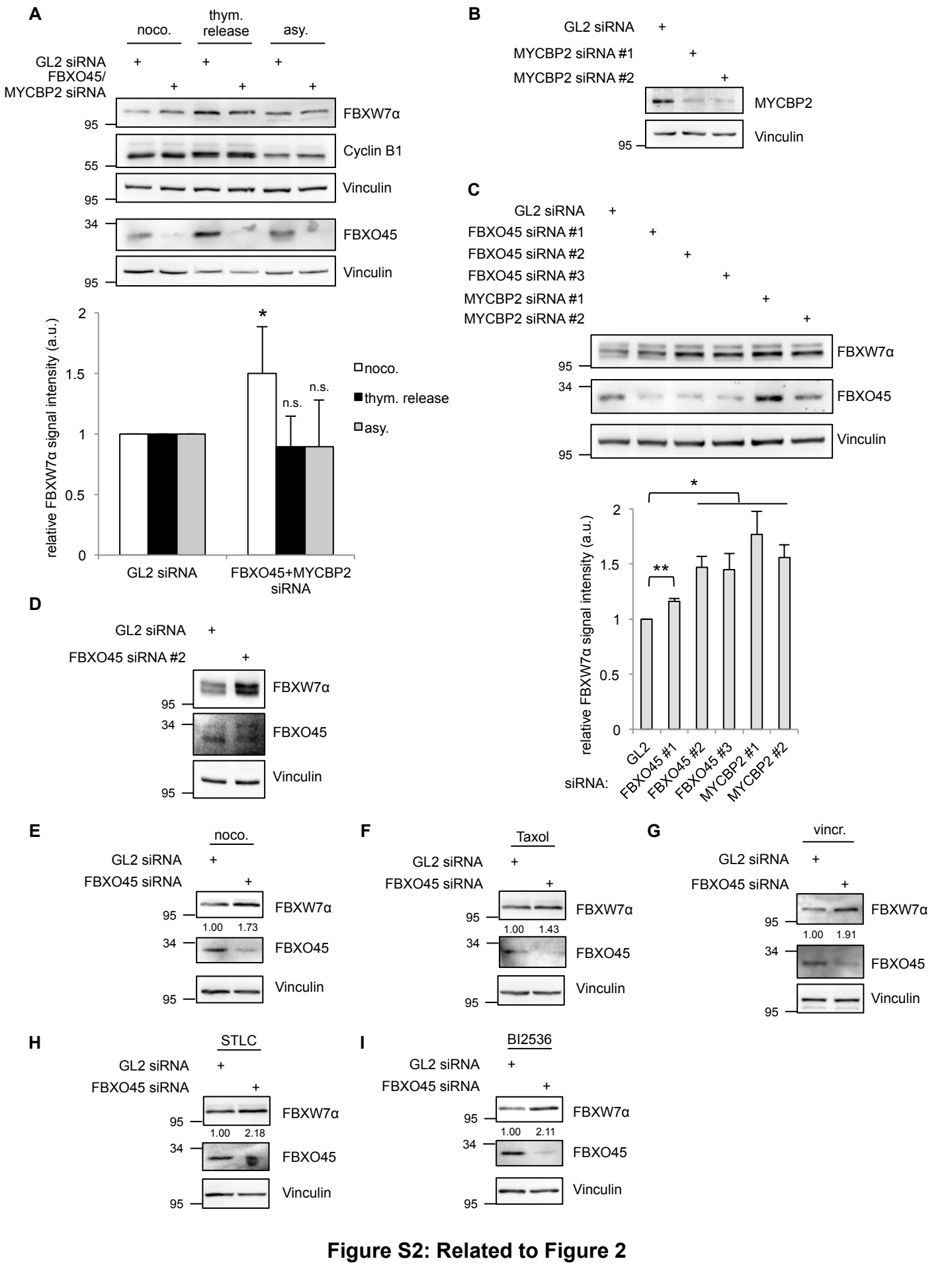

Figure S2: Related to Figure 2

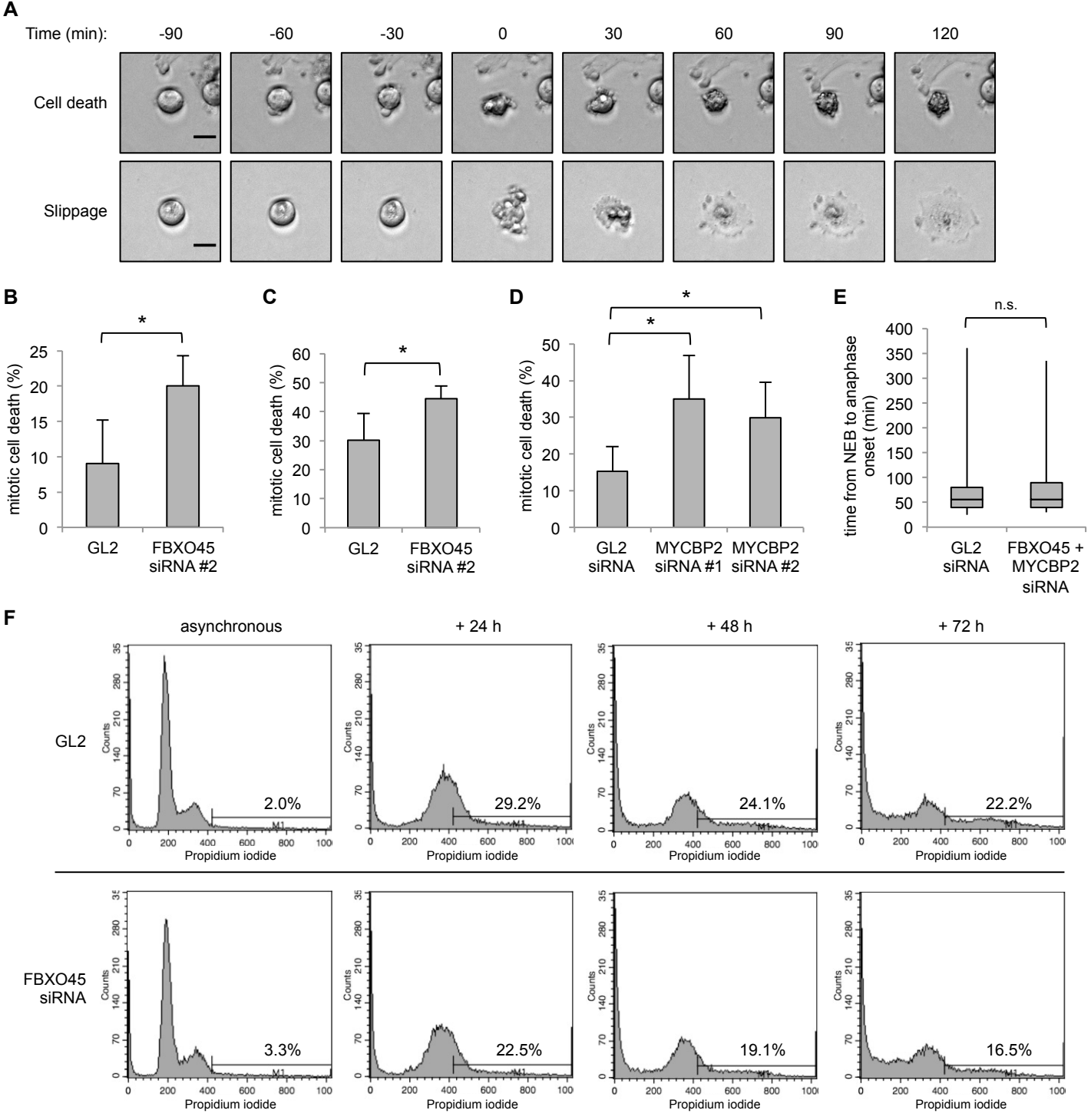

Figure S3: Related to Figure 4